Bulgarian Chemical Communications, Volume 48, Special Issue A (pp. 88 – 94) 2016

Sodium deficient transition metal oxides $Na_{1/2}Co_{1/3}Ni_{1/3}Mn_{1/3}O_2$ as alternative electrode materials for lithium-ion batteries

Sv.G. Ivanova*, E.N. Zhecheva, R.K. Stoyanova

Institute of General and Inorganic Chemistry, Bulgarian Academy of Sciences, Acad. G. Bonchev Str., Bldg. 11, Sofia 1113, Bulgaria

Submitted on July, 17, 2015; Revised on October 23, 2015

Abstract. Sodium-deficient transition metal oxides exhibit flexible layered structures which are able to adopt different layer stacking and symmetry. In this study, we provide new data on the structure and reversible lithium intercalation properties of oxides with composition $Na_{1/2}Co_{1/3}Ni_{1/3}Mn_{1/3}O_2$. Novel properties of oxides determine their potential for using as alternative electrode materials for lithium-ion batteries. Between 700 and 800 °C, new layered oxide $Na_{1/2}Co_{1/3}Ni_{1/3}Mn_{1/3}O_2$ with a *P3*-type of structure is obtained by a precursor-based method. A new structural feature of $Na_{1/2}Co_{1/3}Ni_{1/3}Mn_{1/3}O_2$ as compared to well-known sodium stoichiometric oxides $NaCo_{1/3}Ni_{1/3}Mn_{1/3}O_2$ with an *O*3-type of structure is the development of layer stacking ensuring prismatic site occupancy for Na^+ ions with shared face on one side and shared edges on the other side with surrounding $Co/Ni/MnO_6$ octahedra. The reversible lithium intercalation in $Na_{1/2}Co_{1/3}Ni_{1/3}Mn_{1/3}O_2$ is demonstrated and discussed.

Keywords: Sodium–transition metal–oxides; Layered oxides; Intercalation; Lithium-ion battery

1. INTRODUCTION

Linkage of the intercalation properties with the crystal structure of solids is a research topic that is a basis for recent progress in the design of cathode materials for lithium ion batteries [1]. Among several groups of compounds, layered lithium transition metal oxides are of both research and practical interests since they are able to intercalate lithium reversibly at high potentials [2,3]. Lithium-cobalt-nickel-manganese oxides, $LiCo_{1-2x}Ni_xMn_xO_2$, with compositions x=1/3 have been considered as next generation electrode materials [4]. Contrary to the conventional $LiCoO_2$-based electrodes, $LiCo_{1/3}Ni_{1/3}Mn_{1/3}O_2$ oxides display two electron electrochemical reactions during reversible lithium intercalation, a phenomenon that is generally considered to be rare for layered oxides [5].

Nowdays, lithium ion batteries are the most widely used electrochemical storage systems. However, they are still expensive and are in nonconformity with technical requirements for large scale storage applications [6]. Searching for cheaper energy storage systems, sodium ion batteries have been advanced as an alternative to the lithium ones [6]. Sodium is one of the most abundant elements in the Earth's crust and its redox potential is slightly lower than that for Li, i.e. $E°(Na^+/Na)$= -2.71 V and $E°(Li^+/Li)$= -3.03 V versus standard hydrogen electrode [6]. This means that lithium-ion batteries offer higher power, while sodium ion batteries appear to be cheaper and safer.

Lithium and sodium ion batteries operate by the same mechanism comprising the reversible electrochemical intercalation of Li^+ and Na^+. Recently stoichiometric sodium cobalt nickel manganese oxide $NaCo_{1/3}Ni_{1/3}Mn_{1/3}O_2$ has been proposed as a cathode material for sodium ion batteries [5]. Both $NaCo_{1/3}Ni_{1/3}Mn_{1/3}O_2$ and $LiCo_{1/3}Ni_{1/3}Mn_{1/3}O_2$ analogues have crystal structure composed of discrete $Co_{1/3}Ni_{1/3}Mn_{1/3}O_2$-layers [4,5]. The sodium and lithium ions are sandwiched between the $Co_{1/3}Ni_{1/3}Mn_{1/3}O_2$-layers so as to occupy octahedral sites. Based on the number of the $Co_{1/3}Ni_{1/3}Mn_{1/3}O_2$-layers in the unit cell and the site occupied by Na or Li, the structure of both sodium and lithium analogues is classified as *O3*-type according to notation of Delmas et al. [7].

In order to combine the advantages of lithium and sodium ion batteries, a new concept has recently been proposed [2]. The concept aims at using directly sodium transition metal oxides as electrode materials instead of lithium analogues [3]. This concept is beneficial especially in case of vanadium and manganese-based layered oxides such as $Na_xV_3O_8$, $Na_{2/3}Mn_{1-x}Fe_xO_2$, α-$Na_{0.66}MnO_{2.13}$ and $Na_xNi_{1/2}Mn_{1/2}O_2$.

In this contribution we provide new data on the structure and intercalation properties of sodium deficient cobalt nickel manganese oxides with the aim to analyze their potential usage as cathode materials in lithium-ion batteries. The studies are focused on $Na_xCo_{1/3}Ni_{1/3}Mn_{1/3}O_2$ compositions with x=1/2. For the synthesis of these oxides, we used a

*To whom all correspondence should be sent:
E-mail: svetlana@svr.igic.bas.bg

simple precursor-based method comprising thermal decomposition of mixed acetate-oxalate precursors [8]. The structure and morphology of $Na_{1/2}Co_{1/3}Ni_{1/3}Mn_{1/3}O_2$ are determined by powder X-ray diffraction and SEM analysis. The lithium intercalation in $Na_{1/2}Co_{1/3}Ni_{1/3}Mn_{1/3}O_2$ is carried out in model two-electrode lithium cells of the type Li|$LiPF_6$(EC:DMC)| $Na_{1/2}Co_{1/3}Ni_{1/3}Mn_{1/3}O_2$. The morphology and composition changes during the lithium intercalation are followed by *ex-situ* SEM analysis and laser ablation inductively coupled plasma mass spectrometry (LA-ICPMS).

2. EXPERIMENTAL

$Na_{1/2}Co_{1/3}Ni_{1/3}Mn_{1/3}O_2$ oxides were obtained by oxalate-acetate precursor method. According to this method, sodium hydroxide and oxalic acid were mixed in a molar ratio of 1:1 and ground in an agate mortar until the mixture became sticky. Then solid manganese, nickel and cobalt acetates were added, the molar ratio being Na:Co:Ni:Mn=1/2:1/3:1/3:1/3. Solid residue is treated at 400 ºC, followed by thermal annealing at 700 and 800 °C for 10 hours.

The X-ray structural analysis is made by a Bruker Advance 8 diffractometer with LynxEye detector using CuKα radiation. Step-scan recordings for structure refinement by the Rietveld method are carried out using 0.02° 2θ steps of 4-s duration. The diffractometer point zero, the Lorentzian/ Gaussian fraction of the pseudo-Voigt peak function, the scale factor, the unit cell parameters, the thermal factors, and the line half-width parameters are determined. The computer FullProf Suite Program (1.00) was used in the calculations [9].

The morphology of the precursors and target products is observed by JEOL JSM 6390 scanning electron microscope equipped with an energy dispersive X-ray spectroscopy (EDS, Oxford INCA Energy 350) and ultrahigh resolution scanning system (ASID-3D) in a regime of secondary electron image (SEI). The accelerating voltage is 15 kV and I ~65 A. The pressure is of the order of 10−4 Pa. The electrochemical charge–discharge of $Na_{1/2}Co_{1/3}Ni_{1/3}Mn_{1/3}O_2$ was examined by using two-electrode cells of the type Li|$LiPF_6$(EC:DMC)| $Na_{1/2}Co_{1/3}Ni_{1/3}Mn_{1/3}O_2$. The positive electrode, supported onto an aluminum foil, was a mixture containing 80% of the active composition $Na_{1/2}Co_{1/3}Ni_{1/3}Mn_{1/3}O_2$, 7.5% CNERGY KS 6 L graphite (TIMCAL), 7.5% Super C65 and 5 % polyvinylidene fluoride (PVDF). The electrolyte was a 1 M $LiPF_6$ solution in ethylene carbonate and dimethyl carbonate (1:1 by volume) with less than 20 ppm of water. Lithium electrodes were consisted of a clean lithium metal disk with a diameter of 18 mm. The cells were mounted in a dry box under Ar atmosphere. The electrochemical reactions were carried out using an eight-channel Arbin BT2000 system in galvanostatic mode. The cell is cycled between 1.8 and 4.4 V at C/100, C/20 and C/10 rates. Before the cycling, all cells were relaxed at open circuit for 10 hours.

The compositions of electrodes after the electrochemical reaction were determined by LA-ICPMS. The equipment consists of PerkinElmer ELAN DRC-e ICP-MS and state of the art New Wave UP193FX laser ablation system. The laser beam can analyze spots from 10 microns to 150 μm.

3.RESULTS AND DISCUSSIONS

Figure 1 shows the XRD patterns of $Na_{1/2}Co_{1/3}Ni_{1/3}Mn_{1/3}O_2$ annealed at 700 °C and 800 ºC. All XRD patterns display diffraction peaks that can be assigned to a mixture of the target layered phase and an impurity of NiO-like phase. Therefore, the XRD patterns are calculated based on the structural model that comprises two phases: (i) layered phase with Na in two *3a* sites (0, 0, z_{Na}) and (1/3, 2/3, z_{Na}), Ni/Mn in *3a* sites (0, 0, 0) and oxygen in *3a* sites (0, 0, z_{O1}) and (0, 0, z_{O2}) for a *R3m* space group, and (ii) NiO phase with Ni and O in *4b* (0.5, 0.5, 0.5) and *4a* (0, 0, 0) sites for a space group *Fm-3m*. The amount of NiO impurity is less than 1% and it is insensitive towards the annealing temperature. According to the nomenclature of layered oxides [7], $Na_{1/2}Co_{1/3}Ni_{1/3}Mn_{1/3}O_2$ can be denoted as *P3*-type of structure. The lattice parameters look like slightly dependent on the annealing temperature: a = 2.8299(1) Å and c = 16.7842(14) Å versus a = 2.8308(1) Å and c = 16.7767(14) Å for the oxide annealed at 700 °C and 800 °C, respectively. The lattice volume remains unchanged (116.43 and 116.41 $Å^3$, respectively), thus indicating constancy in the Na content during annealing of the oxides at 700 and 800 °C.

Sodium deficient oxides adopt the *P*3-type of structure, while a well known *O*3-type of structure is stabilized for the sodium stoichiometric oxide $NaCo_{1/3}Ni_{1/3}Mn_{1/3}O_2$. The structural difference between *P*3 and *O*3-modifications comes from the symmetry of the sodium position: In the *P*3-modification all Na^+ ions occupy one prismatic site that shares face on the one side and edges on the other side with the surrounding Co/Ni/MnO_6-octahedra, while one octahedral position for Na^+ ions is available for the *O*3-modification (Fig. 2). It should be mentioned that there is a close structural

relation between *P*3 and *O*3 type structures: by gliding of the $Co_{1/3}Ni_{1/3}Mn_{1/3}O_2$–layers, the *P*3 structure easily transforms to *O*3. The transformation of *O*3 to *P*3 type structure has been reported during the electrochemical extraction of sodium from $NaCo_{1/3}Ni_{1/3}Mn_{1/3}O_2$ [10]. In addition, the O3-modification has been obtained at temperatures higher than 900 °C. This means that the low-temperature synthesis enables to form a new structural modification of sodium deficient oxides $Na_xCo_{1/3}Ni_{1/3}Mn_{1/3}O_2$ with a *P3*-type of structure.

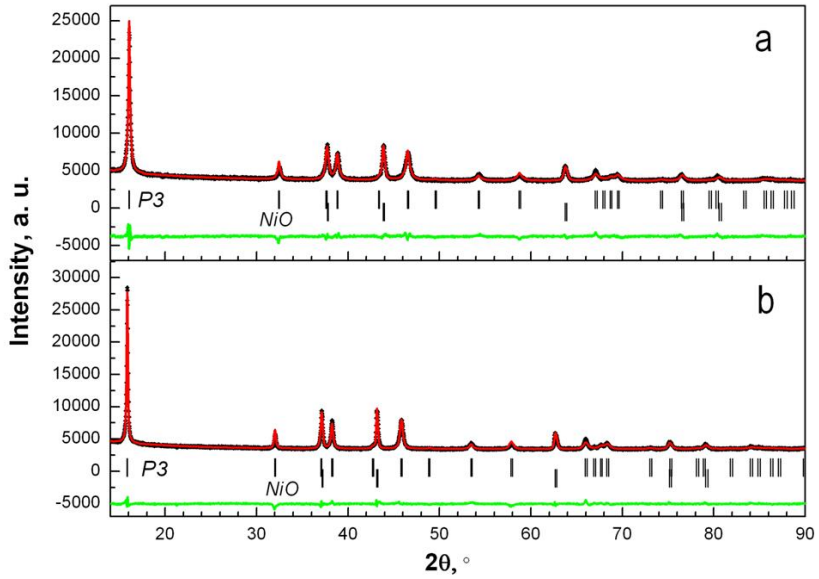

Figure 1. XRD patterns of $Na_{1/2}Co_{1/3}Ni_{1/3}Mn_{1/3}O_2$ annealed at 700 and 800 °C. The Bragg's reflections for *P*3-type of structure are given. The impurity phase (NiO) is also indicated. Dotted lines correspond to the simulated XRD patterns using Rietveld refinement method.

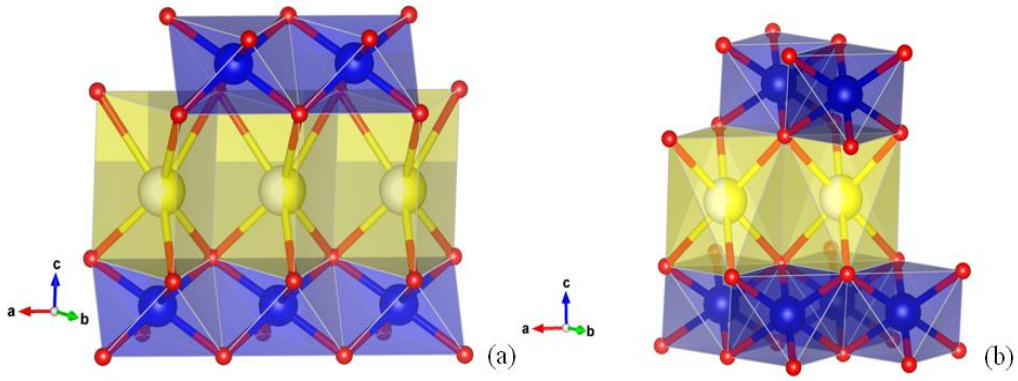

Figure 2. Schematic representation of the sodium position in the *P*3- $Na_{1/2}Co_{1/3}Ni_{1/3}Mn_{1/3}O_2$ and O3- $NaCo_{1/3}Ni_{1/3}Mn_{1/3}O_2$ (*a* and *b*, respectively). Blue and yellow colours correspond to Co/Ni/Mn and Na octahedra, respectively.

The morphology of $Na_{1/2}Co_{1/3}Ni_{1/3}Mn_{1/3}O_2$ annealed at 700 and 800 C is compared on Figure 3. SEM images show the formation of dense aggregates for $Na_{1/2}Ni_{1/2}Mn_{1/2}O_2$, which appears to be insensitive towards the annealing temperature (Fig. 3). EDS analysis demonstrates that all elements are homogeneously distributed over the aggregates. Based on SEM/EDS experiments, the composition of sodium-nickel-cobalt-manganese oxides annealed at 700 °C and 800 °C is shown on Table 1. It is worth mentioning that the chemical composition determined from EDS coincides with that obtained from chemical analysis LA-ICPMS.

3.1. Reversible lithium intercalation in $Na_{1/2}Co_{1/3}Ni_{1/3}Mn_{1/3}O_2$

Comparing the electrochemical performance of oxides annealed at 700 and 800 °C, it appears that good cycling stability is achieved only for $Na_{1/2}Co_{1/3}Ni_{1/3}Mn_{1/3}O_2$ treated at the higher temperature. That is why, all electrochemical

characterization is focused on the oxide annealed at 800 °C.

Figure 4 gives the electrochemical curves for Li^+ intercalation in $Na_{1/2}Co_{1/3}Ni_{1/3}Mn_{1/3}O_2$ at the potential range of 1.8-4.4 V with a charge/discharge rate of C/20 and C/100. When the cell starts with a discharge, a capacity of 157 mAh/g is obtained at a

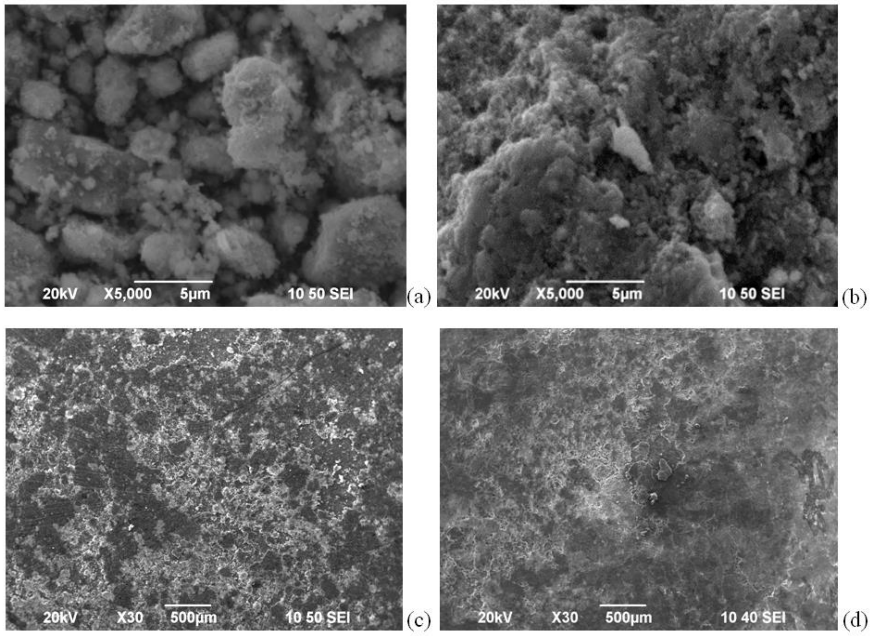

Figure 3. SEM micrographs of $Na_{1/2}Co_{1/3}Ni_{1/3}Mn_{1/3}O_2$ powders annealed at 700 (a) and 800 °C (b). Pristine electrode (c) and electrodes (d) after 10 cycles between 1.8 and 4.4 V at a rate of C/100 and stopped at 4.4V are also given. The electrode comprises a mixture of active oxide $Na_{1/2}Co_{1/3}Ni_{1/3}Mn_{1/3}O_2$ (85%) and 7.5 % graphite, 7.5 % active carbon and 5 % PVDF.

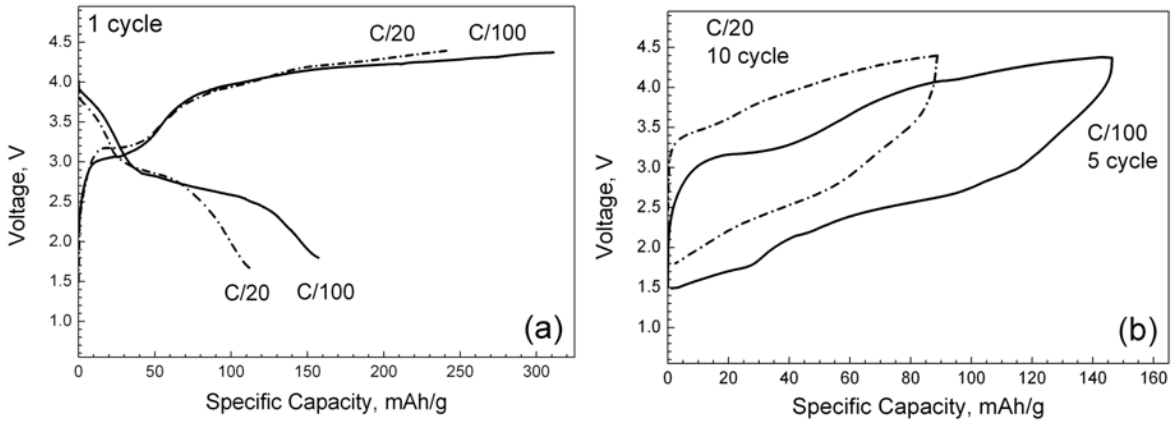

Figure 4. The first discharge and charge curves for $Na_{0.5}Co_{1/3}Ni_{1/3}Mn_{1/3}O_2$ annealed at 800 °C at rates of C/20 and C/100 (a). The cells start with a discharge mode. The charge discharge curves after 5 cycles at a rate of C/100 and after 10 cycles at a rate of C/20 are also presented.

lower rate (i.e. C/100) (theoretical capacity 265.23 mAh/g). By increasing the discharge rate from C/100 to C/20, there is a decrease in the capacity from0 157 to 113 mAh/g. It is noticeable that $Na_{1/2}Co_{1/3}Ni_{1/3}Mn_{1/3}O_2$ delivers the capacity in two potential plateaus of 3.7 and 2.7 V irrespective of the used discharge rate (Fig. 4). This indicates that lithium extraction proceeds with a structural transformation of *P*3- $Na_{1/2}Co_{1/3}Ni_{1/3}Mn_{1/3}O_2$. Supposing that the electrochemical reaction includes only intercalation of Li^+ into the layered $Na_{1/2}Co_{1/3}Ni_{1/3}Mn_{1/3}O_2$ without proceeding of side-reactions between the electrode and the electrolyte, the amount of intercalated Li^+ can be calculated. Thus, the calculated values corresponding to the first discharge capacities at a rate of C/100 and C/20 are 0.62 and 0.44 mol Li per formula unit $Na_{1/2}Co_{1/3}Ni_{1/3}Mn_{1/3}O_2$. It appears that at higher rate (i.e. at C/20), the intercalated amount of Li^+ approaches the sodium deficiency content. It is

noticeable that the amount of Li^+ and Na^+ is slightly lower than 1 (i.e. 0.44+0.50=0.94), which is in an agreement with the structural constrains for the site occupancy by alkali metals in the layered structure: the occupancy is restricted up to 1 mol of alkali ions. When the slow rate is used, the intercalated Li amount is higher than that corresponding to the sodium deficiency content. This means that the added amount of Li^+ and Na^+ ions per formula unit becomes higher than 1 (i.e. 0.62+0.50=1.12). To explain the obvious inconsistency with the structural requirements, one could suppose a possible interaction of the oxide with the electrolyte leading to a preferential Na^+ extraction or partial Li^+/Na^+ exchange.

The analysis of the stability of $Na_{1/2}Co_{1/3}Ni_{1/3}Mn_{1/3}O_2$ in the electrolyte solution is performed by following the change in the voltage

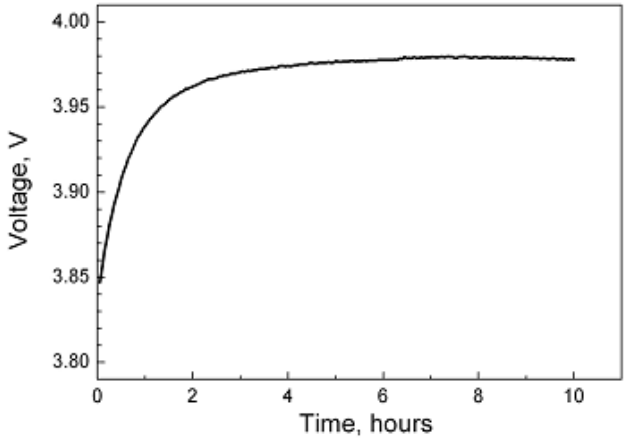

Figure 5. The voltage-time curves for $Na_{1/2}Co_{1/3}Ni_{1/3}Mn_{1/3}O_2$ at open circuit.

of the cell at open circuit (Fig. 5). As one can see, the voltage of the cell increases before the electrochemical reaction, indicating a corresponding rising of the oxidation state of the transition metal ions. The steady state potential is achieved after 3 hours of contact between the electrode and the electrolyte. For the sake of comparison, the voltage of the cell using $LiCo_{1/3}Ni_{1/3}Mn_{1/3}O_2$ analogue as an electrode is stable (not shown). It is important to note that changes in composition of $Na_{1/2}Co_{1/3}Ni_{1/3}Mn_{1/3}O_2$ encompass only the sodium content. Table 1 shows the LA-ICPMS data on the chemical composition of $Na_{1/2}Co_{1/3}Ni_{1/3}Mn_{1/3}O_2$ electrodes after the first discharge down to 2.5 V and 1.8 V. It is clear that the ratio between transition metal ions remains constant during the electrochemical reaction, while the sodium content decreases reaching a value of 0.17. Therefore, the changes in the sodium content and related oxidation states of transition metal ions in $Na_{1/2}Co_{1/3}Ni_{1/3}Mn_{1/3}O_2$ in the electrolyte solution can be regarded as a result from the competition between Na^+ extraction and Na^+/Li^+ exchange reactions. All these reactions can be related with the thermal instability of $LiPF_6$ salt, which is found to decompose to LiF and PF_5 even at room temperature [8]. The reaction product PF_5 has acidic properties and can initiate a series of reactions of Na^+ extraction. For example, acidic PF_5 has been shown to play a crucial role in the formation of the solid electrolyte interphase layer that is composed of organic and inorganic decomposed compounds [8].

During the reverse process of charging, the two-stage intercalation reactions are still distinguished: the two reaction plateaus are shifted to 3.1 and 4.1 V, respectively (Fig. 4). An important issue is that the first charge capacity exceeds the corresponding discharge capacity: 312 and 240 mAh/g for C/100 and C/20, respectively. This means that lithium together with sodium is extracted from the oxide during the first charge process. In addition, a partial exchange of Na^+ with Li^+ cannot be excluded. To analyze the processes of Li^+/Na^+ deintercalation and exchange, Table 1 gives the chemical compositions of electrodes determined by LA-ICPMS.

Table 1. LA-ICPMS and EDS data for chemical composition of $Na_{1/2}Co_{1/3}Ni_{1/3}Mn_{1/3}O_2$ in the form of the powder annealed at 800 °C and in the form of working electrode.

Element	Powder		Pristine electrode	Electrode after the first discharge down to 2.5 V	Electrode after the first discharge down to 1.8 V	Electrode after 10 cycles between 1.8-4.4 V at a rate of C/100	Electrode after 10 cycles between 1.8-4.4 V at a rate of C/10
	LA-ICPMS	EDS	EDS	LA-ICPMS	LA-ICPMS	EDS	EDS
Na	0.52	0.49	0.55	0.25	0.17	0.19	0.12
Mn	0.32	0.34	0.30	0.31	0.31	0.28	0.31
Co	0.33	0.34	0.36	0.32	0.3	0.33	0.37
Ni	0.35	0.32	0.34	0.37	0.39	0.39	0.32

After the first discharge up to 2.5 V (i.e. after Li intercalation), there is a strong increase in the Li-to-Na ratio, which reveals a lowering of the sodium content in the electrodes in comparison with the pristine compositions (Table 1). The extraction of Li^+ ions during the charge process up to 4.4 V is manifested by a consecutive decrease in the Li-to-Na ratio (Table 1). The observed changes in the Li-to-Na ratio imply that partial Li^+/Na^+ exchange reactions starts to develop at the beginning of the Li intercalation (Table 1). Contrary to lithium and sodium, the nickel and manganese content remains constant during the electrochemical reaction (Table 1).

Stable electrochemical performance is achieved after several cycles. Figure 4 gives the charge/discharge curves after 5 cycles at a rate of C/100, as well as after 10 cycles at a rate of C/20. It is obvious that charge/discharge curves become smoother during cycling with Columbic efficiency exceeding 96%. The reversible capacity reaches a value of about 145 and 85 mAh/g for a rate of C/100 and C/20, respectively. This means that the electrochemical reaction takes place through reversible intercalation of about 0.55 and 0.35 mole of Li in the oxides charging and discharging with rates of C/100 and C/20, respectively. The changes in the shape of the charge/discharge curves suggest for structural transformations of *P*3-$Na_{1/2}Co_{1/3}Ni_{1/3}Mn_{1/3}O_2$ occurring during lithium intercalation. On the other hand, the complex form of the electrochemical curves implies that all Ni^{2+}/Ni^{4+}, Co^{3+}/Co^{4+} and Mn^{3+}/Mn^{4+} ionic couples participate in the electrochemical reaction.

Following the structural requirement for restricted site occupancy by alkaline ions, we can suggest that the reversible lithium intercalation is accomplished between two phases: $Na_{x<0.5}Ni_{0.5}Mn_{0.5}O_2$ and $Li_{\sim 0.5}Na_{x<0.5}Ni_{0.5}Mn_{0.5}O_2$ phases, respectively. The possible formation of layered transition metal oxides containing Li^+ and Na^+ in the interlayer space (i.e. $Li_{\sim 0.5}Na_{x<0.5}Ni_{0.5}Mn_{0.5}O_2$) is an interesting finding. In comparison with Na^+ ions, Li^+ ions prefer to reside in octahedral sites only, as a result of which the crystal chemistry for sodium and lithium transition metal oxides is different [12]. However, a good example for the formation of a mixed Li^+/Na^+-oxide are the cobaltates with a composition $Li_{\sim 0.42}Na_{\sim 0.37}CoO_2$ [13]. The structure of $Li_{\sim 0.42}Na_{\sim 0.37}CoO_2$ consists of two alternative AO_2 blocks: a *P2*-type sodium block and an *O3*-type lithium one [12, 13]. Contrary to $Li_{\sim 0.42}Na_{\sim 0.37}CoO_2$, the incorporation of Li into *O3*-$NaNi_{0.5}Mn_{0.5}O_2$ has recently been shown to proceed by the formation of a *P2/O3* intergrowth at an atomic scale [14]. Based on HRTEM analysis, we have demonstrated that lithium intercalation into $Na_xNi_{1/2}Mn_{1/2}O_2$ leads to a structural transformation from the *P3*- to the *O3*-type of structure, where small amount of Na^+ remains in the layered structure and the Li-to-Na ratio is 0.7. In analogy, the structure of mixed Na^+/Li^+-nickel-manganese oxides could be described as composed of *P3* and *O3*-type blocks.

4. CONCLUSION

New sodium-deficient cobalt–nickel–manganese $Na_{1/2}Co_{1/3}Ni_{1/3}Mn_{1/3}O_2$ oxides with a *P*3-type structure are obtained in the temperature range of 700 - 800 °C. The method of synthesis comprises thermal decomposition of mixed acetate-oxalate sodium–transition metal precursors followed by thermal annealing between 700 and 800 °C. Layered oxides $Na_{1/2}Co_{1/3}Ni_{1/3}Mn_{1/3}O_2$ display a reversible lithium intercalation between 1.8 and 4.4 V. During the first discharge of the electrochemical cell up to 1.8 V, Li^+ ions are inserted in the empty sodium positions, leading to the formation of a mixed Li^+/Na^+ oxides $Li_{1-x}Na_xCo_{1/3}Ni_{1/3}Mn_{1/3}O_2$ with a structure that deviates from the pristine layered structure. The electrochemical reaction takes place via structural transformation due to the participation of Ni^{2+}/Ni^{4+}, Co^{3+}/Co^{4+} and Mn^{3+}/Mn^{4+} ionic couples. A partial exchange of Na^+ with Li^+ occurs during the first few cycles, followed by a steady-state performance. The capability of $Na_{1/2}Co_{1/3}Ni_{1/3}Mn_{1/3}O_2$ to intercalate reversibly lithium in high amounts determines their potential for applications in lithium or sodium rechargeable batteries. Although the voltage range and the electrolyte composition are not optimized, it seems that novel compositions $Na_{1/2}Co_{1/3}Ni_{1/3}Mn_{1/3}O_2$ display a satisfactory reversible capacity in a wide potential window, where the reversible capacity of $LiCo_{1/3}Ni_{1/3}Mn_{1/3}O_2$ analogues diminish quickly.

Acknowledgments. *This work was supported by European Social Fund (Grant BG051PO001-3.3.06-0050).*

REFERENCES

1. V. Palomares, P. Serras, I. Villaluenga, K.B. Hueso, J. Carretero-Gonzalez, T. Rojo, *Energy & Environ. Sci.*, **5**, 5884 (2012).
2. S. Bach, J. P. Pereira-Ramos and P. Willmann, *Electrochem. Acta*, **52**, 504 (2006).
3. M. Yoncheva, R. Stoyanova, E. Zhecheva, E. Kuzmanova, M. Sendova-Vassileva, D. Nihtianova, D. 4. Carlier, M. Guignard and C. Delmas, *J. Mater. Chem.*, **22**, 23418 (2012).

5. X. R. Ye, D.Z. Jia, J.Q. Yu, X.Q. Xin, Z. Xue, *Adv. Mater.*, **11**, 941 (1999).
6. M. Sathiya, K. Hemalatha, K. Ramesha, J.-M. Tarascon, A. S. Prakash, *Chem. Mater.*, **24**, 1846 (2012).
6. B. L. Ellis, L. F. Nazar, *Curr. Opin. Solid State Mater. Sci.*, **16**, 168 (2012).
7. C. Delmas, C. Fouassier, P. Hagenmuller, *Phys B+C*, **91**, 81 (1980).
8. Sv. Ivanova, E. Zhecheva, D. Nihtianova, R. Stoyanova, *J. Mater. Sci.*, **46**, 7098 (2011).
9. J. Rodriguez-Carvajal, in: Satellite Meeting on Powder Diffraction of the XV Congress of the IUCr, p. 127 (1990).
10. S. Komaba, N. Yabuuchi, T. Nakayama, A. Ogata, T. Ishikawa, I. Nakai, *Inorg Chem.*, **51**, 6211 (2012).
11. Sv. Ivanova, E. Zhecheva, R. Stoyanova, D. 12. Nihtianova, S. Wegner, P. Tzvetkova, Sv. Simova, *J. Phys. Chem. C*, **115**, 25170 (2011).
12. R. Berthelot, M. Pollet, J. P. Doumerc, C. Delmas, *Inorg. Chem.*, **50**, 6649 (2011).
13. Z. Ren, J. Shen, S. Jiang, X. Chen, C. Feng, Z. A. Xu, G. H. Cao, *Journal of Physics: Condensed Matter*, **18**, L379 (2006).
14. E. Lee, J. Lu, X. Zhang, D. Miller, A. DeWahl, S. Hackney, B. Key, D. Kim, M.D. Slater and C.S. Johnson, *Advanced Energy Materials*, DOI: 10.1002/aenm.201400458.

НАТРИЕВО-ПРЕХОДНОМЕТАЛНИ ОКСИДИ С НЕДОСТИГ НА НАТРИЙ $Na_{1/2}Co_{1/3}Ni_{1/3}Mn_{1/3}O_2$ КАТО АЛТЕРНАТИВНИ ЕЛЕКТРОДНИ МАТЕРИАЛИ ЗА ЛИТИЕВО-ЙОННИ БАТЕРИИ

Св. Г. Иванова*, Е. Н. Жечева, Р. К. Стоянова

Институт по обща и неорганична химия, Българска академия на науките, бул. Акад. Г. Бончев, блок 11, София 1113

Постъпила на 17 юли, 2015 г. коригирана на 23 октомври, 2015 г.

(Резюме)

В тази статия представяме нови данни за структура и обратима интеркалация на литий в оксиди със състав $Na_{1/2}Co_{1/3}Ni_{1/3}Mn_{1/3}O_2$. Натриево-преходнометалните оксиди са синтезирани по оксало-ацетатен метод при 700 и 800 °C, с *P3*-тип структура. Обратима интеркалация на литий се осъществява в потенциалните граници 1.8-4.4 V. По време на първи разряд литиевите йони се интеркалират в незаетите натриеви позиции като се образуват оксиди със състав $Li_{1-x}Na_xCo_{1/3}Ni_{1/3}Mn_{1/3}O_2$, чиято структура е различна в сравнение със структурата на изходните съединения. Електрохимичната реакция се осъществява посредством редокси-двойките Ni^{2+}/Ni^{4+}, Co^{3+}/Co^{4+} и Mn^{3+}/Mn^{4+}. По време на първите няколко цикъла се обменят литиеви и натриеви йони, след което клетката продължава да работи стабилно. Способността на $Na_{1/2}Co_{1/3}Ni_{1/3}Mn_{1/3}O_2$ да интеркалира обратимо литий в големи количества определя потенциалното прилежение на тези оксиди в презареждаеми литиеви и натриеви батерии.